JOURNAL OF THERMOPHYSICS AND HEAT TRANSFER
Vol. 22, No. 3, July–September 2008

Natural Convection Flow in a Cubical Enclosure with a Heated Strip

Esam M. Alawadhi*
Kuwait University, 13060 Safat, Kuwait

DOI: 10.2514/1.36648

Natural convection flow in a cubical enclosure with a heated strip is solved numerically using the finite element method. The heated strip simulates an array of electronic chips. The heated strip is attached to the front wall and maintained at high temperature, and the entire opposite wall is maintained at low temperature. The Rayleigh numbers of 10^4, 10^5, and 10^6 are considered in the analysis and the heated strip is either vertically or horizontally attached to the wall. The results indicate that the heat transfer strongly depends on the orientation and position of the heated strip. The maximum Nusselt number for the horizontal heated-strip configuration can be achieved if the heater is placed at the lower half of the wall, whereas for the vertical heated-strip case, the maximum Nusselt occurs when the heated strip is placed in the middle of the wall. Increasing the Rayleigh number significantly increases heat transfer in the enclosure for the examined case studies.

Nomenclature

a	=	width of the heated strip, m
C_p	=	specific heat, kJ/kg-K
g	=	gravity acceleration, m/s^2
h_s	=	distance from the center of the heated strip to the base wall, m
h_v	=	distance from the center of the heated strip to the left wall, m
k	=	thermal conductivity, W/m-K
L	=	side length of cubical cavity, m
Nu	=	Nusselt number
P	=	pressures, N/m^2
Pr	=	Prandtl number
Ra	=	Rayleigh number
T	=	temperature, K
U, u	=	dimensionless and dimensional x-velocity component, m/s
V, v	=	dimensionless and dimensional y-velocity component, m/s
W, w	=	dimensionless and dimensional z-velocity component, m/s
β	=	thermal expansion, 1/K
θ	=	dimensionless temperature
μ	=	viscosity, N-s/m^2
ν	=	kinematic viscosity, m^2/s
ρ	=	density, kg/m^3
ϕ	=	general field variable

Subscripts

H	=	hot
i	=	iteration number
L	=	cold
m	=	mean

Superscripts

n	=	node number
$*$	=	dimensionless quantity

I. Introduction

THE analysis of the natural convection flow in rectangular air-filled enclosures has expanded recently in the literature due to the important field of applications in thermal management of electronic devices. For cooling chips in cabinets, an array of chips is attached to one of the walls and generates a substantial amount of heat [1,2]. Experimental and numerical analyses of natural convection flow in enclosures have been discussed in great detail in the literature. Numerical simulations of heat transfer in a three-dimensional enclosure with three heaters located at various positions were presented by Chuang et al. [3], and the effect of inclination of the enclosure on the heat transfer was investigated by Tou and Zhang [4]. A cubical enclosure with a square heat source attached to one of vertical walls and cooled by the adjacent walls was studied by Frederick and Berbakow [5]. Their result shows a transition from a conduction- to convection-dominated heat transfer at a Rayleigh number of 10^5, leading to a sharp increase in the overall Nusselt number. A cubical enclosure with a diamond orientation was investigated experimentally by Mamun et al. [6]. The aim of their work was to provide experimental data for computational fluid dynamics (CFD) validation. A cubical enclosure with fins to increase heat transfer was investigated numerically by Frederick and Moraga [7] for Rayleigh numbers of 10^3 to 10^6. Natural convection in a differentially heated cubical enclosure was simulated using the velocity-vorticity form of the Navier–Stokes equations by Lo et al. [8]. They also studied the effect of the inclination of the enclosure in another paper [9]. Natural convection in two-dimensional spaces was also extensively addressed in literature. Natural convection in a rectangular enclosure heated locally from below was accomplished by Sarris et al. [10]. Their results indicated that the position of the heated strip played an important role in the flow, temperature distribution, and thermal penetration, and the effect of the orientation of the enclosure was studied by Jin et al. [11].

Typically, arrays of electronic chips are cooled by natural convection flow [12], especially for low-power applications. Therefore, determining the optimum location for the array is essential for maximizing the heat flow from the chips. The present work studies the natural convection flow in a cubical enclosure with a heated strip attached to one of the vertical walls. The aim of the study is to determine the location for the strip that maximizes the heat transfer. The heated strip simulates an array of electronic chips with finite thickness. The thickness of the chips is negligible compared

Received 14 January 2008; revision received 5 April 2008; accepted for publication 7 April 2008.

*Mechanical Engineering Department, P.O. Box 5969; esam@kuc01.kuniv.edu.kw.

with the size of the electronic device. Additionally, the chips in the array are positioned closely to one another on a board [13]. Hence, considering an array of chips as a strip should be a reasonable approximation. The Rayleigh numbers of 10^4, 10^5, and 10^6 are considered in the analysis and the heated strip is attached either horizontally or vertically to the enclosure in different locations. The width of the heated strip is also studied as a design parameter.

II. Formulation

The geometries considered in the present work are depicted in Fig. 1. A cubical enclosure of sides L contains air, $Pr = 0.71$. The heated strip is attached, either horizontally or vertically, to the front wall at $z = 0$. The width of the heated strip is a. The heated strip is maintained at a uniform high temperature of T_H, and the opposite wall, at $z = L$, is maintained at a uniform low temperature of T_L. All other walls are well insulated. The Rayleigh numbers, ranging from 10^4 to 10^6, are selected to maintain laminar flow [3]. For the case of the horizontal heated strip, the location is varied, ranging from the bottom to top wall, whereas for the vertical heated-strip case, the location is varied from the left to the right wall. Based upon the characteristic scales of L, ν/L, $\rho(\nu/L)^2$, and $T_H - T_L$ and the mean temperature $T_m = (T_H + T_L)/2$, the dimensionless variables are defined as follows:

$$X = x/L \qquad Y = y/L \qquad Z = z/L \qquad U = u/(\nu/L)$$
$$V = v/(\nu/L) \qquad W = w/(\nu/L) \qquad (1)$$
$$P^* = (P + \rho g y)/(\rho(\nu/L)^2) \qquad \theta = (T - T_m)/(T_H - T_L)$$

The geometrical parameters are normalized based on the side length of the cubical cavity (L). The side length of the cubical enclosure is equal to one, and the width of the heated strip is equal to a^*, where $a^* = a/L$. The dimensionless groups relevant to this study are the Rayleigh, Nusselt, and Prandtl numbers, and they are defined, respectively, as

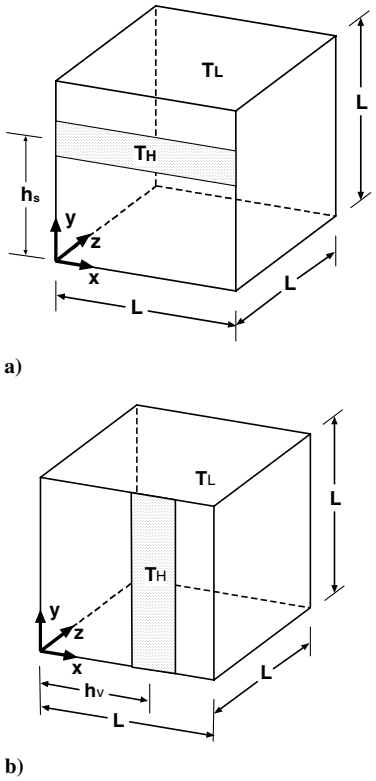

Fig. 1 The cubical enclosure with a) horizontal and b) vertical heated strips.

$$Ra = \frac{g\beta(T_H - T_L)L^3}{\nu^2} Pr \qquad Nu = \frac{hL}{k} \qquad Pr = \frac{\mu C_P}{k} \qquad (2)$$

It is assumed that the viscous dissipation and radiation effects are negligible and the Bussinesq assumption is valid. The governing equations of continuity (3), momentum (4–6), and energy (7) for steady-state, laminar, incompressible flow are as follows:

$$\frac{\partial U}{\partial X} + \frac{\partial V}{\partial Y} + \frac{\partial W}{\partial Z} = 0 \qquad (3)$$

$$U\frac{\partial U}{\partial X} + V\frac{\partial U}{\partial Y} + W\frac{\partial U}{\partial Z} = -\frac{\partial P^*}{\partial X} + \frac{\partial^2 U}{\partial X^2} + \frac{\partial^2 U}{\partial Y^2} + \frac{\partial^2 U}{\partial Z^2} \qquad (4)$$

$$U\frac{\partial V}{\partial X} + V\frac{\partial V}{\partial Y} + W\frac{\partial V}{\partial Z} = -\frac{\partial P^*}{\partial Y} + \frac{\partial^2 V}{\partial X^2} + \frac{\partial^2 V}{\partial Y^2} + \frac{\partial^2 V}{\partial Z^2} + \frac{Ra}{\mathrm{Pr}}\theta \qquad (5)$$

$$U\frac{\partial W}{\partial X} + V\frac{\partial W}{\partial Y} + W\frac{\partial W}{\partial Z} = -\frac{\partial P^*}{\partial Z} + \frac{\partial^2 W}{\partial X^2} + \frac{\partial^2 W}{\partial Y^2} + \frac{\partial^2 W}{\partial Z^2} \qquad (6)$$

$$U\frac{\partial \theta}{\partial X} + V\frac{\partial \theta}{\partial Y} + W\frac{\partial \theta}{\partial Z} = \frac{1}{Pr}\left(\frac{\partial P^*}{\partial X} + \frac{\partial^2 \theta}{\partial X^2} + \frac{\partial^2 \theta}{\partial Y^2} + \frac{\partial^2 \theta}{\partial Z^2}\right) \qquad (7)$$

Because of the elliptic nature of the governing equations, the boundary conditions along the entire domain must be specified for all field variables. The no-slip boundary condition is imposed at the walls of the enclosure. The boundary conditions are as follows:

$$U = V = W = 0 \quad \text{and} \quad \partial\theta/\partial X = 0 \quad \text{at } X = 0$$
$$0 \le Y \le 1 \qquad 0 \le Z \le 1 \qquad (8a)$$

$$U = V = W = 0 \quad \text{and} \quad \partial\theta/\partial X = 0 \quad \text{at } X = 1$$
$$0 \le Y \le 1 \qquad 0 \le Z \le 1 \qquad (8b)$$

$$U = V = W = 0 \quad \text{and} \quad \partial\theta/\partial Y = 0 \quad \text{at } Y = 0$$
$$0 \le X \le 1 \qquad 0 \le Z \le 1 \qquad (8c)$$

$$U = V = W = 0 \quad \text{and} \quad \partial\theta/\partial Y = 0 \quad \text{at } Y = 1$$
$$0 \le X \le 1 \qquad 0 \le Z \le 1 \qquad (8d)$$

For the heated strip,

$$U = V = W = 0 \quad \text{and} \quad \theta = 0.5 \quad \text{at } Z = 0$$
$$0 \le X \le 1 \qquad 0 \le Y \le 1 \qquad (8e)$$

and elsewhere in the wall, $\partial\theta/\partial Z = 0$.

$$U = V = W = 0 \qquad \theta = -0.5 \quad \text{at } Z = 1$$
$$0 \le X \le 1 \qquad 0 \le Y \le 1 \qquad (8f)$$

III. Numerical Method

The dimensionless governing equations combined with the boundary conditions are solved using the finite element method. Brick elements with eight nodes were used to discretized the computational domain. The tridiagonal matrix algorithm iterative

solver [14] was used to solve a set of discretized equations for the three velocity components, and the preconditional generalized minimum residual solver [15] was employed to solve set of discretized equations for pressure and temperature. The advection terms in the momentum and energy equations were formulated by using the streamline upwind Petrov–Galerkin approach [16]. Nithiarasu [17] developed an efficient adaptive mesh regeneration technique for natural convection flow problems, and the listed meshing guidelines were used in the present research.

The relaxation factor of 0.5 was specified for all field variables. The selected solvers and advection formulation with adjacent relaxation factors stabilize the solution toward the convergence. The iterative solver was run until the sum of changes of a field variable calculated from the result between the current iteration and the previous iteration divided by the sum of the current values reached a specific value: $\varepsilon = 10^{-6}$. The convergence criterion has the following form:

$$\frac{1}{\left(\sum_{n=1}^{N} \varphi_n^i\right)} \sqrt{\sum_{n=1}^{N} \left(\varphi_n^i - \varphi_n^{i-1}\right)^2} \le \varepsilon \tag{9}$$

where the superscript i refers to the iteration number, the subscripts n are the node number, ϕ is a field variable, and N is the maximum node number. Decreasing the value of ε below the specified value does not cause significant changes in the result. The three velocity components, pressure, and temperature were calculated. All calculations were carried out using the Intel Xion 3.8-MHz processor workstation, and each simulation took 18.5 h.

Published experimental or numerical data are not available for three-dimensional enclosures with a heated strip similar to that undertaken in the present study. Therefore, a direct validation could not be performed. However, Lo et al. [8] numerically studied a natural convection flow in a cubical enclosure with constant-temperature boundary conditions. In their work, the quadratic differential method is used to solve the problem, and one of the entire vertical walls is maintained at high temperature and the opposite wall is maintained at low temperature. The Lo et al. [8] work is used to ensure that the presented numerical results are accurate enough for engineering applications. For the mesh-sensitivity study, the average Nusselt number is calculated for $Ra = 10^4$, 10^5, and 10^6 using three different mesh sizes: 20^3, 25^3, and 30^3. This test is performed to ensure that the mesh size has no effect upon the final solution. Table 1 shows a comparison between the values of the average Nusselt number obtained using the present finite element code with three mesh sizes and those of Lo et al. The comparison indicates that the results of the present model with a mesh size of 25^3 are in excellent agreement with those of [8]. Therefore, the mesh size of 25^3 is adopted for the present numerical study.

IV. Results and Discussion

In the present problem, the Nusselt number depends on the Rayleigh number and the position of the heated strip. The heated strip is maintained at $\theta_H = 0.5$, and the opposite wall is maintained at $\theta_L = -0.5$. In the first strip configuration, the heated strip is attached horizontally to the front wall at $Z = 0$, and the elevation is varied from the bottom to the top wall, $h_s^* = 0.1 - 0.9$, where $h_s^* = h_s/L$. In the second strip configuration, the heated strip is attached vertically to the front wall at $Z = 0$, and the location is varied from the left to the right wall, $h_v^* = 0.1 - 0.9$, where $h_v^* = h_v/L$. The range of examined Rayleigh numbers is $Ra = 10^4$ to 10^6. Numerical solutions are presented in the form of temperature contours, flow streamlines, velocity profiles, and average Nusselt number. The width of the heated strip a^* is varied between 0.2 and 1. With $a^* = 1$, the entire front wall is heated.

Table 1 Nusselt number for validation and mesh-independent-results study

		Present		
Ra	Lo et al. [8]	20^3 elements	25^3 elements	30^3 elements
10^4	2.251	2.234	2.241	2.241
10^5	4.610	4.512	4.591	4.595
10^6	8.910	8.931	8.910	8.910

A. Temperature Contours and Flow Streamlines

For a qualitative appreciation, temperature contours and flow streamlines at the midplane perpendicular to the front wall are presented for $Ra = 10^5$ and $a^* = 0.2$. Figures 2a–2c show temperature contours on the Y–Z plane at $X = 0.5$, and the heated strip is located at $h_s^* = 0.1$, 0.5, and 0.9, respectively. At the region close to the heated strip, air is raised by buoyancy forces. The moving air has enough momentum to overcome viscous forces at the upper region of the enclosure, where it is forced downward by negative buoyancy forces supplied by the cold wall. The maximum surface temperature occurs at a region close to the heated strip, due to high heat flow from the strip. Also, isotherms are very dense at the region close to the heated strip, compared with the cold wall, showing that a high amount of heat is being released in a small area. With a heated strip located at $h_s^* = 0.1$, Fig. 2a indicates that the air bulk temperature is higher than in the other cases, showing an effective air heating. However, when the heated strip is elevated to $h_s^* = 0.9$ (Fig. 2c), the air bulk temperature is significantly decreased, and the high air temperature is limited to the upper region of the enclosure. For all h_s^* values, the bottom wall is maintained at a temperature close to the cold wall temperature, $\theta_L = -0.5$, because of the cold air flowing from the cold surface. On the other hand, the top wall is maintained at a high temperature because of the hot air flowing from the heated strip. It can be concluded from these figures that installing heat-sensitive electronic components at the bottom wall of the enclosure will be a safe location.

The characteristics of the natural convection flow can be well understood by inspecting the velocity streamlines in the enclosure. The natural convection flow serves an important role in transporting the thermal energy from the heated strip to the cold wall, reducing the thermal resistance in the enclosure and increasing heat transfer. Figures 3a–3c show the flow streamlines on the Y–Z plane at $X = 0.5$ for $Ra = 10^5$, $a^* = 0.2$ and the heated strip located at $h_s^* = 0.1$, 0.5, and 0.9, respectively. In general, these figures show that one clockwise recirculation cell dominates the enclosure, and the location of the center of the cell depends on the h_s^*.

As the heated strip is elevated, the effect of increased buoyancy forces is felt on the flow streamlines. The horizontal and vertical locations of the center of the cell are an indication of the strength of the velocity component in the Y and Z directions, respectively. For all h_s^* values, Fig. 3 indicates that the vertical location of the center of the cell is nearly unaffected by h_s^*, showing that the Y-velocity component is not varying significantly with h_s^*. On the other hand, the horizontal location of the center of the cell is significantly affected by h_s^*, showing that the Z-velocity component is varying significantly with h_s^*. When h_s^* is increased from 0.1 to 0.5 (Figs. 3a and 3b), the center of the recirculation cell is shifted closer to the heated strip, and streamlines become more dense at the region close to the heated strip. When the distance between the streamlines is small, the fluid particles are accelerating along the streamlines. Therefore, the h_s^* is increased from 0.1 to 0.5, and the heat flow from the strip is expected to increase due to the increased heating buoyancy. When h_s^* is increased from 0.5 to 0.9 (Figs. 3b and 3c), the center of the cell is moved away from the heated strip, showing that the air velocity is reduced in the region close to the heated strip.

B. Effect of the Strip Location and Rayleigh Number on the Velocity Profile

The effect of the position of the heater on the Rayleigh number can be explained by studying the velocity profile in the enclosure. Figure 4 shows the velocity profile along a path from $(X, Y, Z) = (0.5, 0.5, 0)$ to $(X, Y, Z) = (0.5, 0.5, 1)$ for $Ra = 10^5$ and $a^* = 0.2$. The Y-velocity component is stronger than other velocity components and represents the main fluid motion in the enclosure.

Air is heated in the region close to the heated strip and moves upward due to the buoyancy force and moves downward in the region close to the cold wall. As the flow approaches the top wall, $Y = 1$, the flow begins to decelerate. On the other hand, in the region close to the cold wall, the flow is downward. Because of the two opposite streams, the

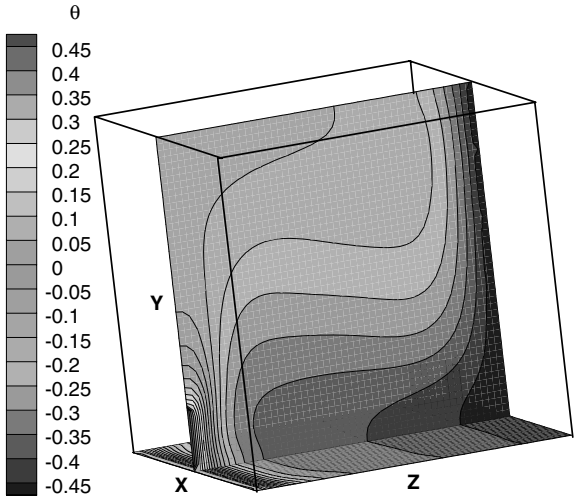

a)

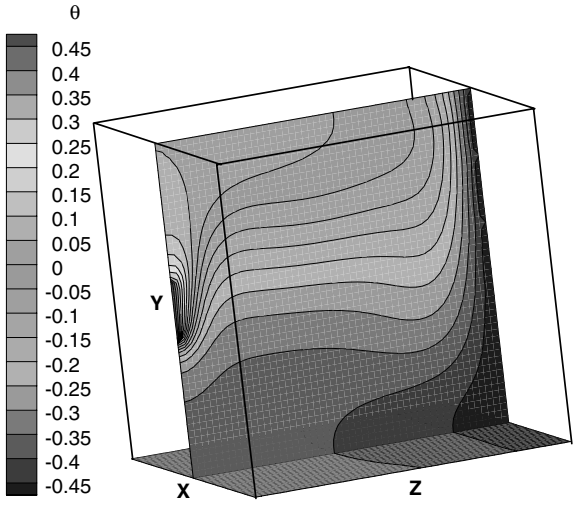

b)

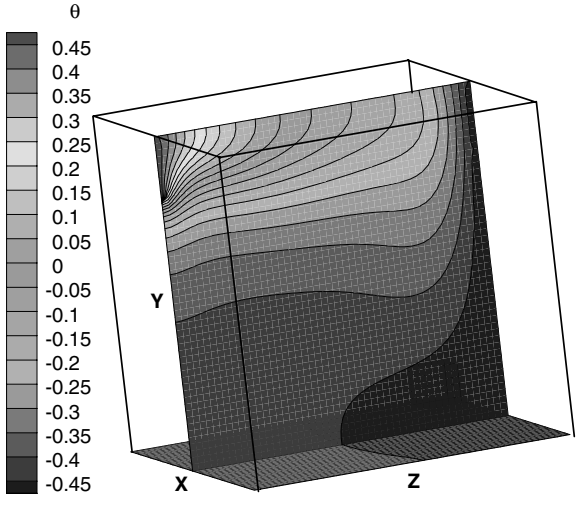

c)

Fig. 2 Temperature contours on the Y–Z plane at $X = 0.5$ for $Ra = 10^5$, $a^* = 0.2$, and the heated strip located at a) $h_s^* = 0.1$, b) $h_s^* = 0.5$, and c) $h_s^* = 0.9$.

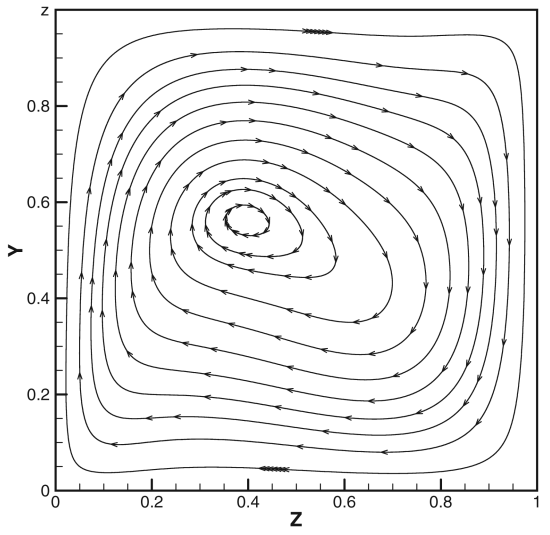

a)

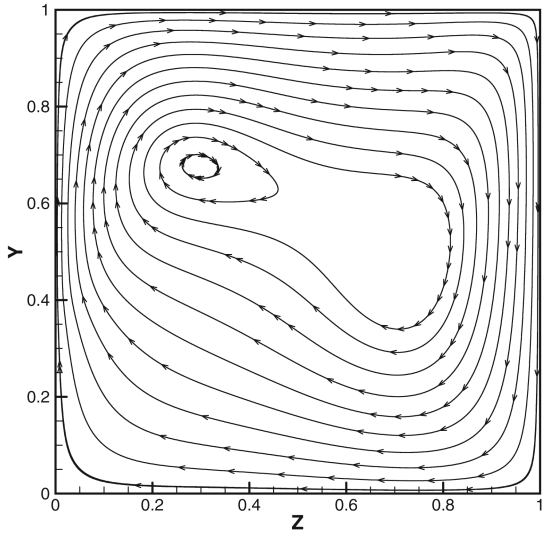

b)

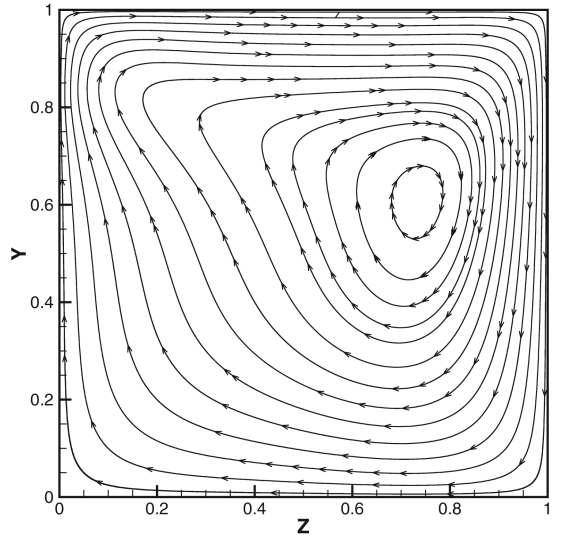

c)

Fig. 3 Velocity streamlines on the Y–Z plane at $X = 0.5$ for $Ra = 10^5$, $a^* = 0.2$, and the heated strip located at a) $h_s^* = 0.1$, b) $h_s^* = 0.5$, and c) $h_s^* = 0.9$.

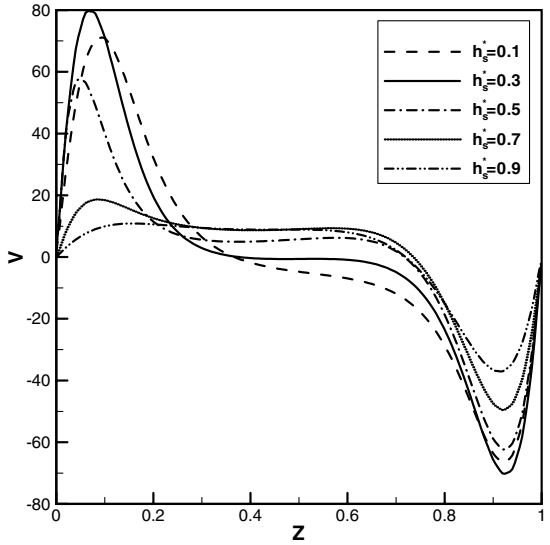

Fig. 4 Velocity profile in the Y direction at different h_s^* values for the horizontal heated-strip configuration for $Ra = 10^5$ and $a^* = 0.2$.

fluid flow is nearly stagnant at the core of the enclosure, as shown in Fig. 4. The vertical position of the heated strip has a noticeable effect on the velocity profile. As the heated strip moves from its minimum height, $h_s^* = 0.1$, the maximum upward velocity increases until it reaches a maximum value at $h_s^* = 0.3$, and then it decreases until the strip is close to the top wall, $h_s^* = 0.9$. When the heated strip is close to the bottom wall, the moving air is unable to take the advantage of the heated strip to gain momentum. Figure 5 shows the effect of the Rayleigh on the velocity profile along a path from $(X, Y, Z) = (0.5, 0.5, 0)$ to $(x, y, z) = (0.5, 0.5, 1)$. The heated strip is located at $h_s^* = 0.3$ and $a^* = 0.2$, and the Rayleigh numbers are 10^4, 10^5, and 10^6. The peak of the Y-velocity component increases with the increase in Rayleigh number due to intensified convection activities. As the Rayleigh number increases, the buoyancy force in the momentum equation increases, which in turn increases the flow velocity. With $Ra = 10^4$, the velocity profile is almost horizontal, and the heat transfer is therefore dominated by conduction mode of heat transfer.

C. Average Nusselt Number Calculations

The overall Nusselt number is obtained by integrating the local Nusselt number at the heated strip. For the horizontal and vertical

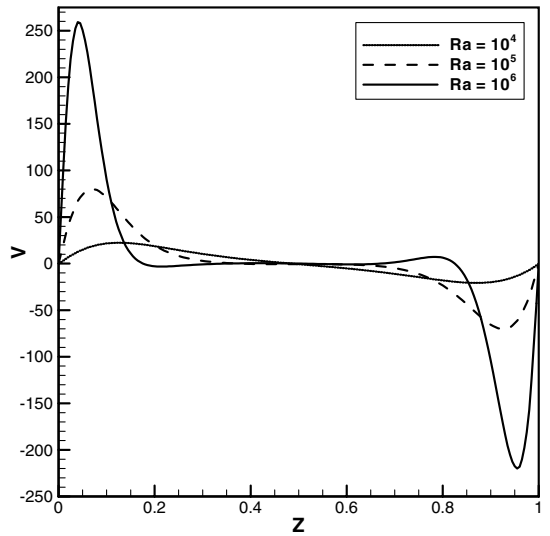

Fig. 5 Velocity profile in the Y direction at different Rayleigh number numbers for the horizontal heated-strip configuration for $h_s^* = 0.3$ and $a^* = 0.2$.

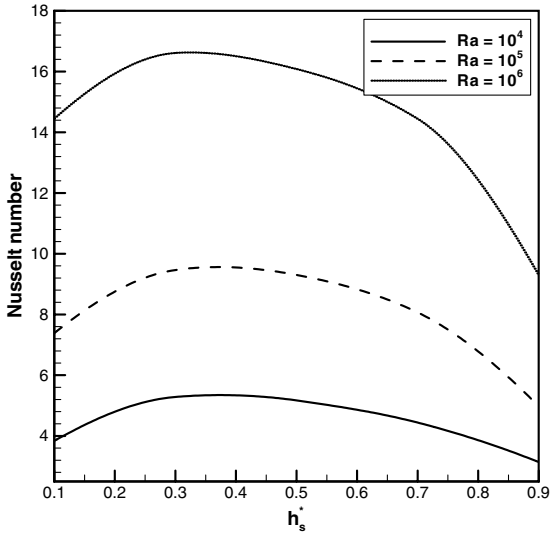

Fig. 6 Effect of the Rayleigh number on the average Nusselt number at the heated strip for $a^* = 0.2$ and the horizontal heated-strip configuration.

heated-strip cases, the average Nusselt numbers are, respectively:

$$Nu = \int_{h_s^*-a^*/2}^{h_s^*+a^*/2} \int_0^1 \frac{1}{\theta_m} \frac{\partial \theta}{\partial Z} \, \mathrm{d}X \, \mathrm{d}Y \tag{10a}$$

$$Nu = \int_{h_v^*-a^*/2}^{h_v^*+a^*/2} \int_0^1 \frac{1}{\theta_m} \frac{\partial \theta}{\partial Z} \, \mathrm{d}Y \, \mathrm{d}X \tag{10b}$$

where θ_m is the air average temperature. Figure 6 shows the effect of the Rayleigh number on the average Nusselt number for $a^* = 0.2$. This figure indicates that for all Rayleigh number values, the average Nusselt number increases from its initial position at $h_s^* = 0.1$ to reach its maximum value and then it decreases again until h_s^* reaches 0.9. Hence, this figure shows that there is an optimum location for the heated strip. The maximum Nusselt number is $h_s^* = 0.375$ for $Ra = 10^4$, $h_s^* = 0.36$ for $Ra = 10^5$, and $h_s^* = 0.325$ for $Ra = 10^6$. With the optimum h_s^*, the thermal resistance in the enclosure is a minimum, and the heat flow is therefore maximized. For $Ra = 10^5$, changing the position of the heater from $h_s^* = 0.1$ to 0.36 increases the Nusselt number by 28%. On the other hand, for $Ra = 10^6$, changing the position of the heater from $h_s^* = 0.1$ to 0.325 increases the Nusselt number by 15%. At a given h_s^* value, increasing the Rayleigh number increases the average Nusselt number. The Nusselt number grows very slowly with h_s^* at low values of Rayleigh number, showing a predominantly conductive heat transfer regime. Conversely, for high values of Rayleigh number, the Nusselt number increases markedly with h_s^*, showing a strong influence of the natural convection flow. For example, for $h_s^* = 0.3$, increasing the Rayleigh number from 10^4 to 10^6 increases the Nusselt number by 211%. A numerical correlation for the Nusselt number as a function of Rayleigh number and h_s^* is presented in the following expression:

$$Nu = 2.302 e^{-2.237 h_s^*} h_s^{*0.691} Ra^{0.255} \tag{11}$$

Correlation (11) produces a maximum percentage error of 6.23%. The average Nusselt number at the vertical heated strip is calculated using Eq. (10b). Figure 7 shows the effect of Rayleigh number on average Nusselt number for $a^* = 0.2$, and the h_v is varied from 0.1 to 0.9. A symmetric variation of Nusselt number is observed in the figure, as expected. This figure indicates that the position of the heated strip and Rayleigh number have a significant effect on the Nusselt number. With an increase in Rayleigh number, the buoyancy force increases resulting in strong natural convection inside the enclosure. For all Rayleigh number values, the Nusselt number increases as the symmetry plane is approached, and the maximum value of the Nusselt number occurs at $h_v^* = 0.5$. For $Ra = 10^5$,

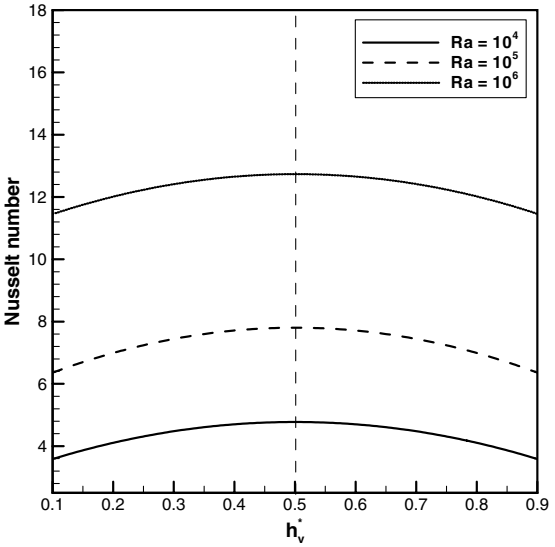

Fig. 7 Effect of the Rayleigh number on the average Nusselt number at the heated strip for $a^* = 0.2$ and the vertical heated-strip configuration.

changing the position of the strip from $h_v^* = 0.1$ to 0.5 increases the Nusselt number by 16%. When the heated strip is at the center of the wall, the air is able to expand and maximize its velocity, and the adjacent vertical walls act as an obstacle for the natural convection flow. For $h_v^* = 0.5$, increasing the Rayleigh number from 10^4 to 10^6 increases the Nusselt number by 176%. A numerical correlation for the Nusselt number as a function of Rayleigh number and h_v^* is presented in the following expression:

$$Nu = 1.086e^{-0.91h_v^*}h_v^{*0.347}Ra^{0.231} \tag{12}$$

Correlation (12) produces a maximum percentage error of 4.42%. For other heated-strip widths, Table 2 shows the effect of the heated-strip width on the average Nusselt number for the horizontal and vertical configurations. For both configurations, the heated strip is located at the middle of the wall, $h_s^* = h_v^* = 0.5$, and its width is increased from $a^* = 0.2$ to 0.6 and 1. For all examined cases, increasing the magnitude of a^* decreases the average Nusselt number for all Rayleigh number values. Increasing the magnitude of a^* increases the surface area of the heated strip, which consequently reduces the heat flux out of the heated strip. For $a^* = 1$, the horizontal and vertical configurations are the same, and the results become close to those of [8].

D. Dimensional Example

To provide the reader with a better sense of scale of the present problem, an example with dimensions is illustrated. Consider a cubical enclosure with the following geometrical parameters: $L = 0.1$ m, $h_s = 0.03$ m, and $a = 0.02$ m. The temperatures of the heated strip and the cold wall are 29.538 and 20°C, respectively. The working fluid is air. With these inputs, the Rayleigh number is 10^6, and the heat transfer coefficient is equal to 4.253 W/m-K. If the heated-strip temperature is decreased to 20.953°C, the Rayleigh number will be 10^5, and the heat transfer coefficient is equal to 2.422 W/m-K.

Table 2 Nusselt number for different heated-strip thicknesses

	Horizontal heated strip			Vertical heated strip		
Ra	$a^* = 0.2$	$a^* = 0.6$	$a^* = 1$	$a^* = 0.2$	$a^* = 0.6$	$a^* = 1$
10^4	5.168	2.873	2.241	4.679	2.750	2.241
10^5	9.301	5.775	4.595	7.601	5.310	4.595
10^6	16.078	10.743	8.910	12.545	9.798	8.910

V. Conclusions

Natural convection flow in a cubical enclosure with a heated strip is presented. The heated strip is attached to the front wall and maintained at high temperature, and the entire opposite wall is maintained at low temperature. The Rayleigh numbers, ranging from 10^4 to 10^6, are considered in the analysis, and the heated strip is either vertically or horizontally attached to the enclosure at different locations. The results indicate that the heat transfer strongly depends on the position and orientation of the heated strip. The result shows that there is an optimum location for the heated strip that maximizes the heat transfer. For the horizontal heated strip, the optimum location is found to be at the lower half of the wall. Changing the elevation of the heated strip can increase the Nusselt number by 28%. For the vertical heated-strip case, the maximum Nusselt occurs when the heated strip is placed in the middle of the wall. Increasing the Rayleigh number significantly increases heat transfer in the enclosure for the examined case studies. Increasing the magnitude of heated-strip width decreases the average Nusselt number for all Rayleigh number values.

References

[1] Liu, Y., and Phan-Thien, N., "An Optimum Spacing Problem for Three Chips Mounted on a Vertical Substrate in an Enclosure," *Numerical Heat Transfer*, Pt. A, Vol. 37, No. 6, May 2000, pp. 613–630. doi:10.1080/104077800274118

[2] Heindel, T., Ramadhyani, S., and Incropera, F., "Conjugate Natural Convection from an Array of Protruding Heat Sources," *Numerical Heat Transfer*, Pt. A, Vol. 29, No. 1, Jan. 1996, pp. 1–18. doi:10.1080/10407789608913775

[3] Chuang, S., Chiang, J., and Kuo, Y., "Numerical Simulation of Heat Transfer in a Three-Dimensional Enclosure with Three Chips in Various Position Arrangements," *Heat Transfer Engineering*, Vol. 24, No. 2, Mar. 2003, pp. 42–59. doi:10.1080/01457630304076

[4] Tou, S., and Zhang, X., "Three-Dimensional Numerical Simulation of Natural Convection in an Inclined Liquid-Filled Enclosure with an Array of Discrete Heaters," *International Journal of Heat and Mass Transfer*, Vol. 46, No. 1, Jan. 2003, pp. 127–138. doi:10.1016/S0017-9310(02)00253-3

[5] Frederick, R., and Berbakow, O., "Natural Convection in Cubical Enclosure with Thermal Sources on Adjacent Vertical Walls," *Numerical Heat Transfer*, Pt. A, Vol. 41, No. 3, Feb. 2002, pp. 331–340. doi:10.1080/10407780252780199

[6] Mamun, M., Leong, W., Hollands, K., and Johnson, D., "Cubical-Cavity Natural Convection Benchmark Experiments: An Extension," *International Journal of Heat and Mass Transfer*, Vol. 46, No. 19, Sept. 2003, pp. 3655–3660. doi:10.1016/S0017-9310(03)00155-8

[7] Frederick R., and Moraga, S., "Three-dimensional Natural Convection in Finned Cubical Enclosures," *International Journal of Heat and Fluid Flow* (to be published).

[8] Lo, D., Young, D., and Murugesan, K., "GDQ Method for Natural Convection in a Cubical Cavity Using Velocity-Vorticity Formulation," *Numerical Heat Transfer*, Pt. B, Vol. 48, No. 4, Oct. 2005, pp. 363–386. doi:10.1080/10407790591009251

[9] Lo, D., Young, D., Murugesan, K., Tsai, C., and Gou, M., "Velocity-Vorticity Formulation for 3D Natural Convection in an Inclined Cavity by DQ Method," *International Journal of Heat and Mass Transfer*, Vol. 50, Nos. 3–4, Feb. 2007, pp. 479–491. doi:10.1016/j.ijheatmasstransfer.2006.07.025

[10] Sarris, I., Lekakis, I., and Vlachos, N., "Natural Convection, in Rectangular Tanks Heats Locally from Below," *International Journal of Heat and Mass Transfer*, Vol. 47, Nos. 14–16, July 2004, pp. 3549–3563. doi:10.1016/j.ijheatmasstransfer.2003.12.022

[11] Jin, L., Tou, K., and Tso, C., "Effects of Rotation on Natural Convection Cooling from Three Rows of Heat Sources in a Rectangular Cavity," *International Journal of Heat and Mass Transfer*, Vol. 48, Nos. 19–20, Sept. 2005, pp. 3982–3994. doi:10.1016/j.ijheatmasstransfer.2005.04.013

[12] Ju, Y., and Chen, Z., "Numerical Simulations of Natural Convection in an Enclosure with Discrete Protruding Heaters," *Numerical Heat Transfer*, Pt. A, Vol. 30, No. 2, July 1996, pp. 207–218.

doi:10.1080/10407789608913836

[13] Madhavan, P., and Sastri, V., "Conjugate Natural Convection Cooling of Protruding Heat Sources Mounted on a Substrate Placed Inside an Enclosure: A Parametric Study," *Computer Methods in Applied Mechanics and Engineering*, Vol. 188, Nos. 1–3, July 2000, pp. 187–202.
doi:10.1016/S0045-7825(99)00147-4

[14] Patankar, S., *Numerical Heat Transfer and Fluid Flow*, Hemisphere, Washington, D.C., 1980.

[15] Jaroslav, M., "Finite Element and Boundary Element Applied in Phase Change, Solidification and Melting Problem. A Bibliography (1996-1998)," *Finite Elements in Analysis and Design*, Vol. 32, No. 3, June 1999, pp. 203–311.
doi:10.1016/S0168-874X(99)00007-4

[16] Brooks, A., and Hughes, T., "Streamline Upwind/Petrov-Galerkin Formulation for Convection Dominated Flows with Particular Emphasis on the Incompressible Navier-Stokes Equation," *Computer Methods in Applied Mechanics and Engineering*, Vol. 32, Nos. 1–3, Sept. 1982, pp. 199–259.
doi:10.1016/0045-7825(82)90071-8

[17] Nithiarasu, P., "An Adaptive Remeshing Technique for Laminar Natural Convection Problem," *Heat and Mass Transfer*, Vol. 38, No. 3, Feb. 2002, pp. 243–250.
doi:10.1007/s002310100228